

LABORATORY EXPERIMENTS AND NUMERICAL MODELS OF INTERACTING EXPLOSIONS

P. F. Velázquez,^{1,4} H. Sobral,² A. C. Raga,¹ M. Villagrán-Muniz,² and R. Navarro-González³

Received 2001 February 12; accepted 2001 April 4

RESUMEN

Presentamos resultados de experimentos de laboratorio y de simulaciones numéricas, donde se analiza la interacción entre dos explosiones. En el laboratorio, estas ondas de choque son generadas focalizando los haces de dos láseres de Nd:YAG, produciendo ondas expansivas en el aire. Las simulaciones se llevaron a cabo empleando el código *yguazú-a* (Raga et al. 2000).

Mostramos que las simulaciones numéricas y los experimentos de laboratorio coinciden de forma satisfactoria, y describimos las propiedades generales de los flujos resultantes. Finalmente, discutimos las similitudes y diferencias entre los experimentos de láser en laboratorios y algunos objetos astrofísicos.

ABSTRACT

We present laboratory experiments and numerical simulations of the interaction between two explosions. In the laboratory, two expanding shock waves were produced using two Nd: YAG lasers, and the numerical simulations were carried out with the *yguazú-a* code (Raga et al. 2000).

We show that the numerical simulations and laboratory experiments agree in a satisfactory way, and we discuss the general properties of the resulting flows. Finally, we discuss the similarities and differences between the laboratory experiments and some astrophysical objects.

Key Words: HYDRODYNAMICS — ISM: SUPERNOVA REMNANTS — METHODS: LABORATORY — METHODS: NUMERICAL — SHOCK WAVES

1. INTRODUCTION

Recently, laser laboratory experiments are being employed as a new tool to study complex astrophysical phenomena (such as the propagation of shock waves, the development of hydrodynamic instabilities, and the evolution of jets and supernova remnants) and also to validate astrophysical gasdynamic codes. For example, Kane et al. (1997) carried out laboratory laser experiments in order to study hydrodynamical instabilities (such as the Richtmyer-Meshkov and Rayleigh-Taylor instabilities), under conditions which are relevant for supernovae, using the Nova Laser at Lawrence Livermore National Lab-

oratory (LLNL). They also compare their laboratory results with simulations performed with different codes (HYADES, CALE, and PROMETHEUS, see Kane et al. 1997).

Keilty et al. (2000) carried out experiments in which a Petawatt laser at LLNL (with an energy of 1 kJ) is focused on a target of CH material. Furthermore, they carried out simulations with the HYADES code, considering different radii (from 1 to 20 μm) for the energy deposition region. They conclude that the radius of the blast waves are independent of the original sizes of the energy deposition region, as expected from the self-similar nature of evolved strong explosions.

Teyssier, Ryutov, & Remington (2000) study the possibility of creating stratified atmospheres in laboratory conditions employing high-energy lasers. Decreasing density gradients are a common feature in

¹Instituto de Astronomía, Universidad Nacional Autónoma de México.

²Centro de Instrumentos, Universidad Nacional Autónoma de México.

³Instituto de Ciencias Nucleares, Universidad Nacional Autónoma de México.

⁴Postdoctoral Fellow of CONICET, Argentina.

astrophysics (being of great importance in many astrophysical objects such as supernova explosions, accretion disks, etc.). They designed two experiments: in the first one, a two density step package, which was made with three layers (solid plastic of density $\rho_1 = 1 \text{ g cm}^{-3}$, plastic foam with $\rho_2 = 10 \text{ mg cm}^{-3}$, and penthene gas with $\rho_3 = 0.1 \text{ mg cm}^{-3}$); and in the second experiment a stratified atmosphere of $20 \mu\text{m}$ width was generated by indirect illumination of a plastic target by a thin gold foil. In this experimental setup, Teyssier et al. (2000) study the mechanism of shock acceleration and the stability of shock fronts propagating into a medium with a decreasing density profile.

Raga, Navarro-González, & Villagrán-Muniz (2000) and Sobral et al. (2000) carried out experiments of expanding, laser generated plasma bubbles, and compared the experimental results with gasdynamic numerical simulations. These experiments and simulations are relevant in an astrophysical context, as they provide an opportunity to study the flow resulting from anisotropic explosions, which are expected to occur astrophysical situations such as novae (see e.g., Lloyd et al. 1993).

The laboratory experiments described in the papers referenced above are interesting in that they provide information that is complementary to the one obtained in usual theoretical and/or observational studies. For example, the experimental results permit a direct evaluation of the accuracy of astrophysically oriented gasdynamic codes. This evaluation can be done with flows of strong qualitative resemblance to astrophysical flows, rather than with much more simple flows which have complete analytic solutions. In the recent past, we have carried out evaluations of gasdynamic codes involving quantitative comparisons with experimental time series of aspherical explosions (Raga et al. 2000; Sobral et al. 2000) and of low Mach number jets (Raga et al. 2001). It is clearly not possible to obtain such evaluations of gasdynamic simulations through comparisons with astrophysical objects since the boundary conditions of the astrophysical flows are not well known, and in general one does not have detailed observational time series for most astrophysical flows.

In the present paper we extend the work of Raga et al. (2000) and Sobral et al. (2000) to study interactions between two explosions. We do this by carrying out experiments with two laser generated plasma bubbles, which result in a pair of interacting shock waves. We then compare the resulting flows with results from numerical simulations with appropriate parameters. Finally, we discuss the similarities and

differences between our laboratory flows and some astrophysical flows.

2. THE LASER EXPERIMENT

A sketch of the experimental setup is shown in Figure 1. The double explosion was done by focusing the beams of two Q-switched Nd:YAG lasers (Continuum, model Surelite II) with two plane-convex lens with focal lengths of 5 and 7.5 cm (lens L1 and L2, Fig. 1), respectively. The lasers are operated at $\lambda = 1.06 \mu\text{m}$ and 10 Hz repetition rate, with a 7 ns pulse width (FWHM) and 6 mm beam diameter. Two experiments were carried out: in the first experiment, the energies were 500 and 50 mJ, while in the second one, the same energy was employed in both lasers (300 mJ). The laser energies were measured employing two energy meters (Lab-Master Ultima with crystalline pyroelectric sensor LM-P10i from Coherent) EM1 and EM2 through two calibrated beam splitters BS1 and BS2 (see Fig. 1). Both laser pulses were synchronized by means of a Stanford delay generator model DG-535 (DG1 in Fig. 1).

The region where the laser beams are focused was illuminated with an expanded He-Ne laser beam ($\lambda = 632.8 \text{ nm}$, JDS Uniphase model 1125P and a power of 10 mW). After passing through the region of interest, the probe beam was imaged with an ICCD 1024×256 camera (PI-MAX:1024UV from Princeton Instruments) with a gate width of less than 5 ns, and the signal was stored in a PC. This camera was synchronized with the laser pulses using another Stanford delay generator (DG2 in Fig. 1).

With this experimental setup, we obtained shadowgrams at a series of different times-delays with respect to the two synchronized Nd:YAG laser pulses. These shadowgrams reveal the structure of the interacting shock waves, which we then compare with results from numerical simulations.

3. NUMERICAL SIMULATION AND COMPARISON WITH LASER EXPERIMENTS

Figures 2 and 3 show the shadowgrams obtained for a series of different time delays in two of our “double explosion” experiments. In the experiment shown in Fig. 2, the input laser energies were of 500 and 50 mJ (left and right bubbles, respectively), and in the experiment shown in Fig. 3 the two laser pulses had an energy of 300 mJ each. The fact that at early times the two expanding shock waves have different shapes in the latter (equal energy) experiment is a

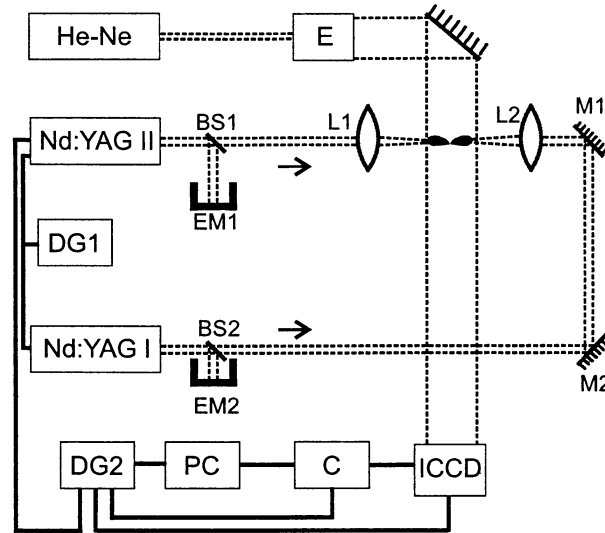


Fig. 1. Experimental setup of the laser-generated interacting shock waves. The employed notation is the following: **E** (expansor), **L1** and **L2** (lens), **M1** and **M2** (mirrors), **BS1** and **BS2** (beam splitters), **EM1** and **EM2** (energy meters), **ICCD** (intensified CCD camera), **DG1** and **DG2** (delay generators) and **C** (controller).

result of the different focal lengths of the two lenses with which the lasers are focused (see § 2).

Also shown in Figs. 2 and 3 are the density stratifications obtained from numerical simulations with initial conditions appropriate for the corresponding experiments. The initial conditions for the simulations are set as follows.

In previous papers (Raga et al. 2000; Sobral et al. 2000), we have shown that the expanding shock wave formed by a laser generated plasma bubble can be well reproduced by numerical simulations with a “hot cone” initial condition (see Figure 4). An initial temperature $T_c = 25,000$ K is imposed inside a conical region, and the length l and half-opening angle α are chosen by trial and error in such a way that the computed shape of the expanding shock wave reproduces the experimental results. In this way, we have chosen two cones with $\alpha_1 = \alpha_2 = 15^\circ$ and $l_1 = 4.8$ mm, $l_2 = 2.2$ mm for the first experiment (see Figs. 2 and 4), and $\alpha_1 = 15^\circ$, $\alpha_2 = 10^\circ$, $l_1 = 4$ mm, $l_2 = 5.3$ mm for the second experiment (see Figs. 3 and 4).

For the two simulations, we consider that two explosions occur simultaneously in a homogeneous and isotropic atmosphere with density $\rho_0 = 10^{-3}$ g cm $^{-3}$ and a temperature $T_0 = 300$ K (approximately corresponding to the conditions found in México City, at 2100 m above sea level).

Furthermore, different distances d , between the vertices of the two “hot cones” were tried in or-

der to simulate the laser experiment pictures. The best agreement with the experimental results was obtained for $d_1 = 4.6$ mm and $d_2 = 4.8$ mm for the first and second experiments, respectively (see Fig. 4).

With these initial conditions, we integrated the cylindrically symmetric gasdynamic equations using the *yquazú-a* code, which is described in detail by Raga et al. (2000). This code uses a second order algorithm based on the flux vector splitting method of Van Leer (1982), and works with a hierarchical, binary adaptive grid. For our simulations, we have used a 5-level binary adaptive grid with a maximum resolution of 5.9×10^{-3} cm, in a 3×1.5 cm (axial \times radial) full computational domain.

Figs. 2 and 3 show the density stratifications obtained at different times from the simulations of our two experiments. Each of the two explosions produces an outwardly expanding shock wave (which we will call the “principal shock waves” PSW1 and PSW2). These shock waves have initial Mach numbers ranging from $M = 2 \rightarrow 5$.

From $t = 0$ to $3 \mu\text{s}$, we can see that the PSW1 and PSW2 shock waves propagate into the surrounding medium. These two shock waves collide with each other at $t \approx 3$ and $4 \mu\text{s}$ (for the first and second experiments, respectively, see Figs. 2 and 3). This shock collision produces a high pressure interaction region which drives two reflected shock waves (RSW1 and RSW2) traveling back towards the centers of each of the two explosions. The gas in be-

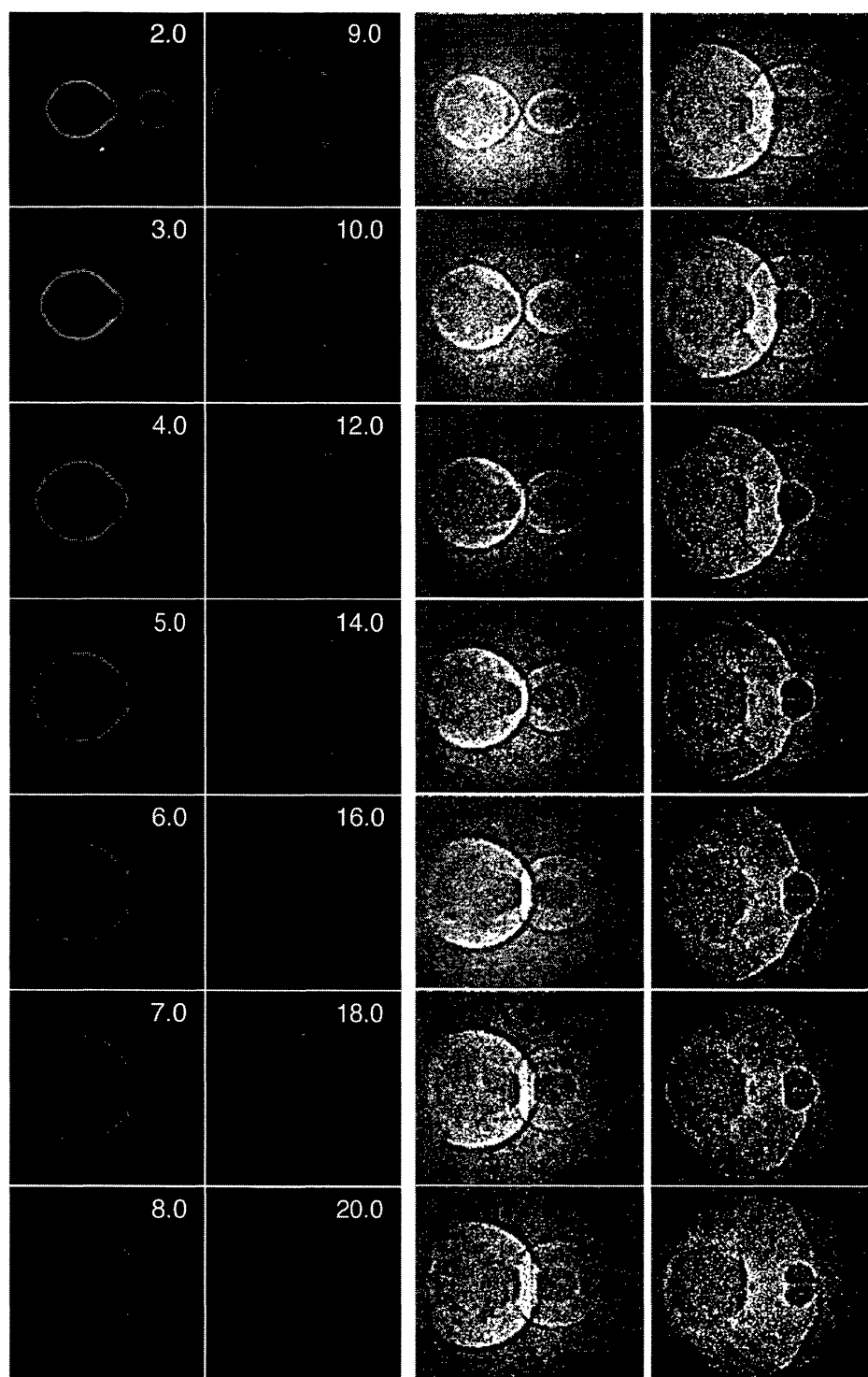


Fig. 2. Comparison between a numerical simulation and an experiment of two laser generated explosions (with input energies of 500 and 50 mJ). The two left columns correspond to density stratifications obtained from our simulation (each frame is labeled with the time in μs). The gray-scale varies between 5×10^{-5} and 1 g cm^{-3} . The second two columns show the shadowgrams obtained from the laser experiment, for the same times as the corresponding graphs of the first two columns. All of the frames have a vertical size of 2.5 cm.

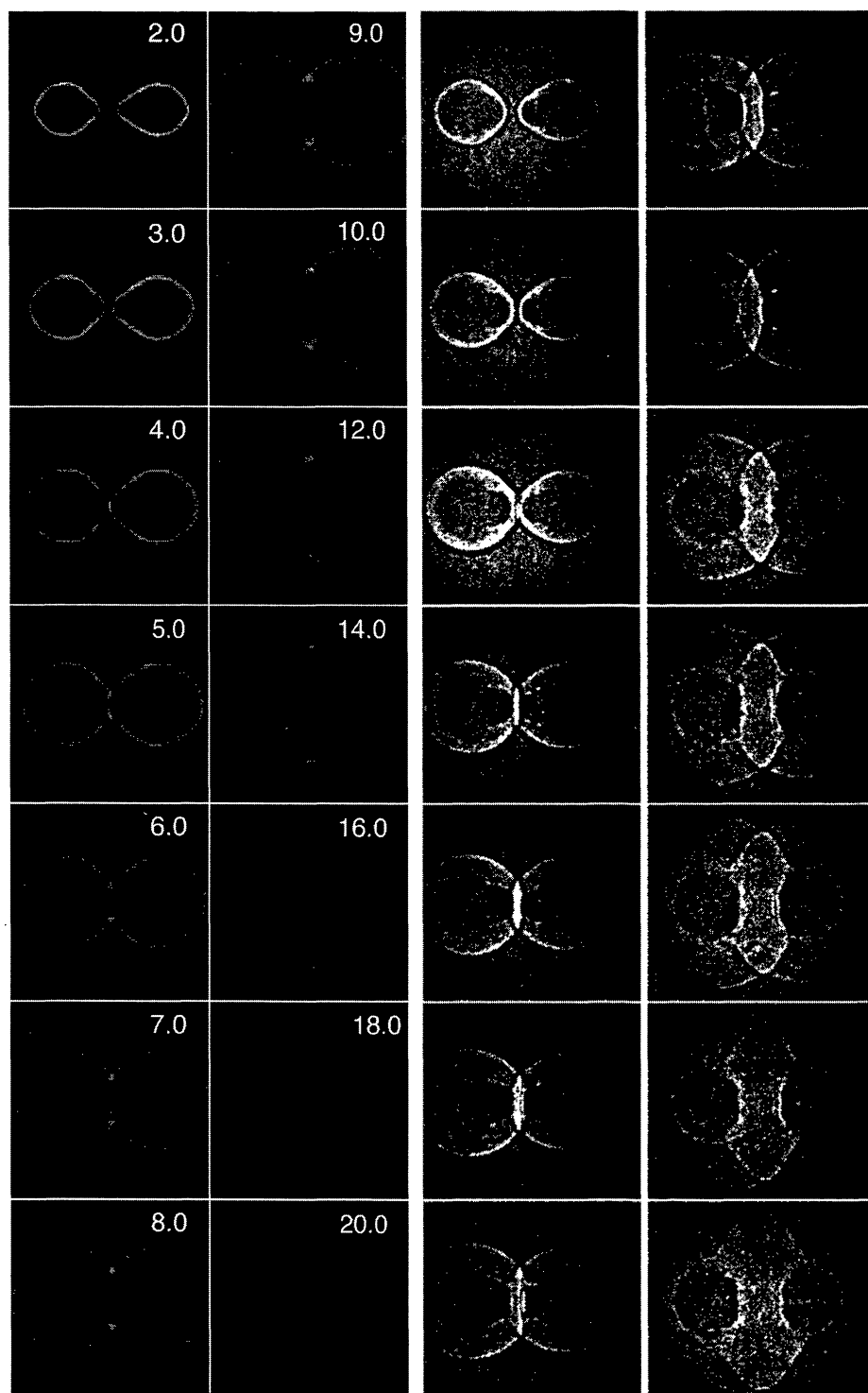


Fig. 3. The same as Figure 2, but for an experiment with two explosions produced by lasers of equal energy (300 mJ).

tween RSW1 and RSW2 initially has a temperature of ≈ 400 K, and cools adiabatically quite rapidly, regaining an ≈ 300 K, atmospheric temperature at a time $t \approx 8 \mu\text{s}$.

RSW1 and RSW2 propagate into gas which has been previously shocked by the PSW1 and PSW2 shocks, respectively. The on-axis regions of the reflected shocks eventually collide (at $t \approx 5 \mu\text{s}$ for both experiments) with the hot, low density bubbles (which correspond to the material which was initially heated by each of the two laser pulses). The regions of RSW1 and RSW2 which propagate within the hot air bubbles become weak compression waves, which are not clearly visible in the flow stratifications of neither the numerical simulations nor the experiments. These compression waves push the hot air bubbles away from each other, as can be clearly seen from the increasing size of the gap between the two bubbles for times $t = 8 \rightarrow 20 \mu\text{s}$. While in the equal energy case the two gas bubbles have almost identical recoils (see Fig. 3), in the first, unequal energy experiment, the gas bubble resulting from the low energy laser pulse shows a stronger recoil (see Fig. 2).

From Figs. 2 and 3 we see that the parts of RSW1 and RSW2 which do not interact with hot gas bubbles continue moving into the gas which was swept up by PSW1 and PSW2. The two principal and the two reflected shock waves all meet at a single point (which actually corresponds to a ring due to the cylindrical symmetry of the flow). The high compression produced at this point results in the formation of a high density ring which expands away from the symmetry axis.

Interestingly, there is a clear qualitative difference between the shadowgrams and the predicted density stratifications. In the shadowgrams one sees the regions of high temperature/density gradients (across the line of sight) as curves defined by contiguous bright and dark features. This is due to the change in refraction index at these surfaces, which results in different refractions of the imaging laser light on each side of the discontinuity. Homogeneous regions are seen as featureless, grey areas in the shadowgrams, with the level of grey being independent of the value of the density of the region.

In the greyscale depictions of the density stratification obtained from the numerical simulation, the discontinuities are clearly seen (see Figs. 2 and 3), as well as other properties of the flow (such as the contrast between the low density of the hot bubble and the higher density of the surrounding environment) which are not seen in the shadowgrams. In order

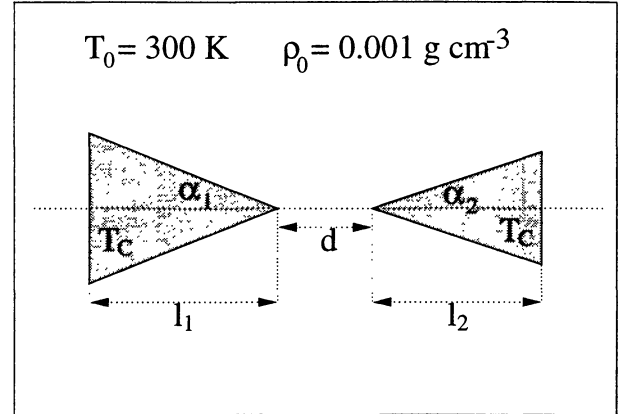


Fig. 4. Schematic diagram showing the initial conditions for the numerical simulation of two interacting shock waves, produced by focusing the beams of two Nd:YAG lasers. The computational domain has a 3×1.5 cm (axial \times radial) size, and a uniform, $\rho_0 = 10^{-3} \text{ g cm}^{-3}$ initial density is imposed over all of the domain. The plasma bubbles produced by the two synchronized laser pulses are modeled as two co-axial cones of lengths $l_{1,2}$, half-opening angles $\alpha_{1,2}$, and temperature $T_c = 25,000$ K, with a separation d between the vertices of the two cones. A $T_0 = 300$ K temperature was imposed in the region outside the two cones.

to produce predictions from the numerical simulations which fully model the observed shadowgrams, it is necessary to solve a complex, variable refraction index radiative transfer problem. However, it is possible to produce predictions that qualitatively resemble the shadowgrams by computing maps of the Laplacian of the density field (through the midplane of the cylindrically symmetric flow). An example of this is shown in Fig. 3, where we show the map of the Laplacian of the density field for the equal explosion energy model, for a $t = 9 \mu\text{s}$ time integration. This map can be compared with the corresponding shadowgram showed in Fig. 3.

4. CONCLUSIONS

We have carried out laboratory experiments and numerical simulations of the interaction between two laser-generated plasma bubbles. We find a convincing agreement between the simulations and the experimental results for cases with equal or different input laser energies.

From the point of view of astrophysical flows, it is interesting to note that the dimensionless numbers of our laboratory experiments are approximately in the appropriate regime. For example, the Reynolds number of the flow (calculated with the initial size of

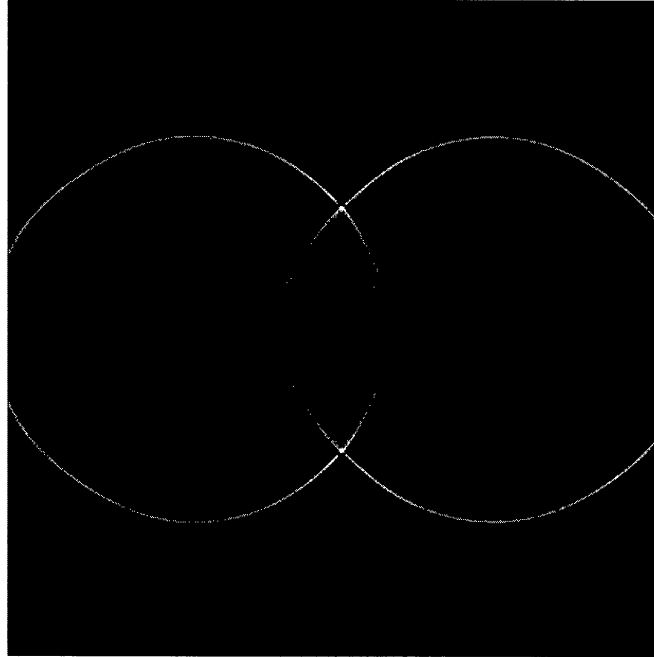


Fig. 5. Laplacian of the density field for the equal explosion energy model, for a $t = 9 \mu\text{s}$ integration time. This figure can be compared with the corresponding shadowgram shown in Fig. 3 (the top frame of the right column).

the plasma bubbles) has a value $Re \sim 10^5$, placing the experiments in the high Reynolds number regime (which is also the appropriate regime for astrophysical flows). The Mach numbers of our experiments have $M \approx 5$ values in the initial states of the evolution of the explosions, but have decayed to $M \approx 2$ (for $t \approx 5 \mu\text{s}$) by the time that the two shock waves interact. Therefore, the Mach numbers of the interacting shock waves are considerably smaller than the $M \sim 10 \rightarrow 100$ values appropriate for supernova explosions.

Notwithstanding this difference in Mach number between our experiment and astrophysical flows, it is interesting to note that some interacting SNR's show morphologies that do resemble our laboratory experiments. For example, the emission line images and radio continuum maps of DEM L316 in the Large Magellanic Cloud (Murphy-Williams et al. 1997) show a structure that qualitatively resembles the $t = 6$ or $7 \mu\text{s}$ frames from our first, "unequal energy explosions" experiment (see Fig. 2). Quite remarkably, both the radio maps and the [O III] 5007 image show a ring-like intensity enhancement in the "neck" of the hourglass shape of DEM L316. In our experiments and numerical simulations, this region shows a ring-like density enhancement (see § 3), in qualitative agreement with the observations.

Finally, we should note that our study of interacting explosions serves as a new test of our "yguazú-a" adaptive grid gasdynamic code. Clearly, our code is able to reproduce interacting explosions in a satisfactory way, and can be used to reliably compute this kind of flow for other initial conditions. We will use this positive result for a future numerical study of interacting SNR's or of a SNR expanding in a stratified interstellar medium (Velázquez et al. 2001), in which we will do a more complete and detailed analysis of interacting shock waves, extending the previous numerical work of Ikeuchi (1978), Jones et al. (1979), Bodenheimer, Yorke, & Tenorio-Tagle (1984) and Tenorio-Tagle, Bodenheimer, & Yorke (1985).

We thank an anonymous referee for useful comments, which helped us to improve a previous version of this paper. PV and AR acknowledge support from CONACyT grants 32753-E and 27546-E. AR acknowledges support from a fellowship of the John Simon Guggenheim Memorial Foundation. HS and MV acknowledge support from CONACyT 33956 and DGAPA IN107600 grants. RN acknowledges support from DGAPA-UNAM IN119999 and CONACyT 32531-T grants.

REFERENCES

- Bodenheimer, P., Yorke, H. W., & Tenorio-Tagle, G. 1984, *A&A*, 138, 215
- Ikeuchi, S. 1978, *PASJ*, 30, 563
- Jones, E. M., Smith, B. W., Straka, W. C., Kodis, J. W., & Guitar, H. 1979, *ApJ*, 232, 129
- Kane, J., Arnett, D., Remington, B. A., Glendinning, S. G., Castor, J., Wallace, R., Rubenchik, A., & Fryxell, B. A. 1997, *ApJ*, 478, L75
- Keilty, K., Liang, E., Remington, B., London, R., Estabrook, K., & Kane, J. 2000, *ApJS*, 127, 375
- Lloyd, H. M., Bode, M. F., O'Brien, T. J., & Kahn, F. D. 1993, *MNRAS*, 265, 457
- Murphy-Williams, R., Chu, You-Hua, Dickel, J. R., Beyer, R., Petre, R., Smith, R. C., & Milne, D. K. 1997, *ApJ*, 480, 618
- Raga, A. C., Navarro-González, R., & Villagrán-Muniz, M. 2000, *RevMexAA*, 36, 67
- Raga, A. C., Sobral, H., Villagrán-Muniz, M., Navarro-González, R., & Masciadri, E. 2001, *MNRAS*, in press
- Sobral, H., Villagrán-Muniz, M., Navarro-González, R., & Raga, A. C. 2000, *Applied Phys. Letters*, v77(n20), 3158
- Tenorio-Tagle, G., Bodenheimer, P., & Yorke, H. W. 1985, *A&A*, 145, 70
- Teyssier, R., Ryutov, D., & Remington, B. 2000, *ApJS*, 127, 503
- Van Leer, B. 1982, ICASE Report No. 82-30
- Velázquez, P. F., de la Fuente, E., Rosado, M., & Raga, A. C. 2001, in preparation

Alejandro C. Raga and Pablo F. Velázquez: Instituto de Astronomía, UNAM, Apartado Postal 70-264, 04510 México, D. F., México (raga,pablov@astrosmo.unam.mx).

Hugo Sobral and Mayo Villagrán-Muniz: Centro de Instrumentos, UNAM, Apartado Postal 70-186, 04510 México, D. F., México (martins.mayo@aleph.cinstrum.unam.mx).

Rafael Navarro-González: Laboratorio de Química de Plasmas y Estudios Planetarios, Instituto de Ciencias Nucleares, UNAM, Apartado Postal 70-543, 04510, México, D. F., México (navarro@nuclecu.unam.mx).